

Eigenstate plateau transition and equilibration in 1D quantum lattice models

Wei-Han Li^{1,*} and Abbas Ali Saberi^{2,1,†}

¹Max Planck Institute for the Physics of Complex Systems, 01187 Dresden, Germany

²Department of Physics, University of Tehran, P. O. Box 14395-547, Tehran, Iran

We report on a remarkable spectral phenomenon in a generic type of quantum lattice gas model. As the interaction strength increases, eigenstates spontaneously reorganize and lead to plateaus of the interaction energy, with gaps opening akin to continuous phase transitions. Perturbation theory identifies a hidden structure underlying eigenstates within each plateau, resulting in a statistical shift in the wavefunction amplitudes described by extreme value theory. The structured eigenstates manifest themselves naturally in far-from-equilibrium dynamics proceeding through multiple universal stages. Our findings reveal a profound connection between emergent properties in high-energy states and out-of-equilibrium dynamics, providing insights into the impact of interactions across the entire energy spectrum. The results are directly relevant to experiments probing equilibration in quantum spin and lattice gases.

Introduction.— The study of quantum many-body systems has mainly focused on their equilibrium properties and low-energy characteristics, particularly the ground states and associated quantum phase transitions. However, exploring the exotic out-of-equilibrium phenomena and in the vast high-energy realms delves into fundamental questions that are still unanswered. Recent years have seen a burgeoning interest in exploring the equilibration dynamics of closed quantum systems [1, 2], particularly in low dimensions, propelled by the advances in ultracold atomic experiments [3–5]. This progress has enabled the realization of archetypal model Hamiltonians [6–9] and the ability to study dynamical equilibration phenomena such as mass expansion [10–14] and spin transport [15, 16] in highly controllable settings. A key frontier has been the exploration of long-range interacting quantum gases [17], where strong inter-site interactions can be engineered in optical lattices, giving rise to effective long-range spin models [18–20] and extended Hubbard models (EHMs) [21–23]. The delicate interplay between these tunable interactions and kinetic energy in such systems can cause novel quantum phases [24–27] and rich non-equilibrium dynamical behavior [28–32].

For various one-dimensional (1D) EHMs and spin models, previous studies have revealed that inter-site interactions strong enough to drive ground-state phase transitions can induce intriguing changes in dynamical properties. These include a qualitative slowdown of quench dynamics [23], distinct features in the self-return probability [34], and transitions in far-from-equilibrium transport behavior [35, 36]. In this letter, we consider a generic 1D EHM, which can be mapped to the XXZ model (spin- $\frac{1}{2}$ Heisenberg chain). Our main focus lies in exploring the emergent properties of the many-body eigenstates arising from the tunable inter-site interactions and identifying their signatures in the out-of-equilibrium dynamics.

We uncover a hidden structure across the spectrum as inter-site interactions increase, where eigenstates exhibit plateaus of interaction energies. The gaps between these plateaus serve as order parameters in

continuous phase transitions, remaining stable upon extrapolation to infinite system size and displaying power-law scaling. Using perturbation theory, we identify a structure shared among eigenstates within each plateau, our arguments also predict statistical shifts in the distribution of eigenstates described by extreme value theory. Although probing the structure of an eigenstate with specific energy may be impossible in a thermodynamic system, the structures across the full spectrum impact far-from-equilibrium dynamics that involve numerous eigenstates. We study the time evolution of Fock states, revealing multiple equilibration stages that universally apply across different interaction forms in current experiments. Our findings offer deeper insights into previous theoretical studies [34–36] and a recent experimental observation [23].

The model.— We consider the EHM described by the Hamiltonian

$$H = \sum_j -t (\hat{a}_{j+1}^\dagger \hat{a}_j + \hat{a}_j^\dagger \hat{a}_{j+1}) + V \hat{n}_{j+1} \hat{n}_j, \quad (1)$$

where \hat{a}_j^\dagger (\hat{a}_j) is the creation (annihilation) operator at lattice site j and $\hat{n}_j = \hat{a}_j^\dagger \hat{a}_j$ is the on-site occupation with the hard-core constraint $(\hat{a}_j^\dagger)^2 = 0$. We assume periodic boundary conditions, and half filling, $N/L = \frac{1}{2}$, for N particles moving in L sites.

Equation (1) is a generic model capturing 1D quantum lattice gases that emphasize nearest-neighbor (NN) interactions. The interplay between the hopping amplitude t and the interaction strength $|V|$ is the core factor influencing the eigenstates. A well-known example is the quantum phase transition [33] when the EHM is mapped onto the XXZ model [44]. For $|V|/t > 2$, the ground state turns from paramagnetic to ferromagnetic or antiferromagnetic depending on the sign of V . Nonetheless, an increase in $|V|$ does not merely impact the ground state; in principle, the influence extends to all excited states in the spectrum.

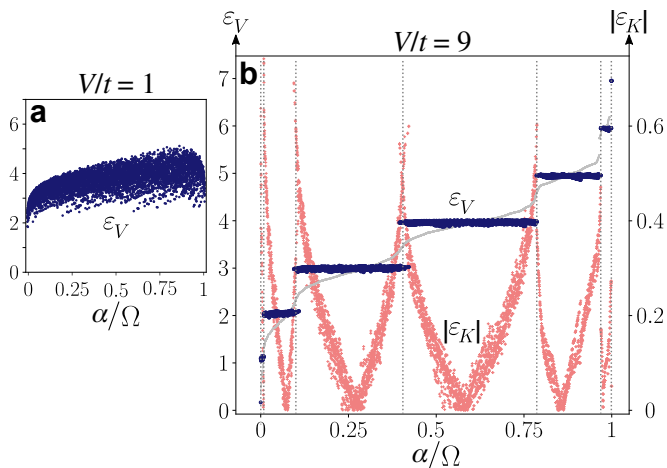


FIG. 1: Emergence of plateaus. The scaled interaction energy ε_V (blue symbols) for the eigenstates labeled by $\alpha = 1, \dots, \Omega$ sorted in ascending order of total energy ε . Where Ω is the dimension of the Hilbert space for $N/L = 8/16$. (a) The continuum of ε_V for $V/t = 1$. (b) The discrete plateaus of ε_V for $V/t = 9$, while ε (gray solid line) remains continuous. High mobility indicated by the high modulus of the kinetic energy $|\varepsilon_K|$ (red symbols) appears at the two sides of each plateau. Vertical dotted lines are the boundaries of plateaus for $t = 0$.

Observables and parameters. Our study focuses on the response of excited states to V , the control parameter. Hence we take $\partial H/\partial V = \hat{l}$ as a response parameter of interest, where

$$\hat{l} = \sum_j \hat{n}_{j+1} \hat{n}_j, \quad (2)$$

is the number of NN links. The ferromagnetism (antiferromagnetism) mentioned above thus corresponds to the extreme expectation value $\langle \hat{l} \rangle \rightarrow N - 1$ ($\langle \hat{l} \rangle \rightarrow 0$). Additionally, states with the same $\langle \hat{l} \rangle$ may have different numbers of solitary particles or holes, e.g., $\bullet \bullet \bullet \circ \circ \circ$ and $\bullet \circ \circ \circ \bullet \bullet$. These particles and holes are given as

$$\hat{s} = \sum_j (\hat{n}_{j+1} - 1) \hat{n}_j (\hat{n}_{j-1} - 1) + \hat{n}_{j+1} (\hat{n}_j - 1) \hat{n}_{j-1}, \quad (3)$$

where the first and second term denotes the solitary particles and holes, respectively.

A solitary particle in Eq. (3) can move freely when no links are altered, as in the case of $\circ \bullet \circ \circ \leftrightarrow \circ \circ \bullet \circ$. Similar motion occurs for a hole when one link is broken and another is created, as in $\bullet \bullet \circ \bullet \leftrightarrow \bullet \circ \bullet \bullet$. Through these motions, a solitary particle can turn into a solitary hole and vice versa, for example, $\bullet \bullet \circ \bullet \circ \bullet \circ \bullet \leftrightarrow \bullet \bullet \bullet \circ \bullet \circ \bullet \circ \bullet \leftrightarrow \bullet \bullet \bullet \bullet \circ$. Therefore, double counting between the solitary particles and holes must be avoided, and as shown in the Supplementary Information (SI), their total number is constrained. From now on, we will refer to the solitary particles and holes together as *singlons*.

The motions of singlons conserve \hat{l} and \hat{s} . From the perturbation point of view, large $|V|$ renders an

eigenstate governed by a set of Fock bases that are mutually connected through the motion of singlons. We consider these bases to share a *common structure*, as each of them can be "mapped" to all the others through singlon motions and vice versa [45]. These common structures are identified by Eq. (2) and (3); they are non-local parameters that classify the eigenstates. We will take Eq. (2) as our main indicator.

Plateau transitions.— Let us first examine the energetic response of the eigenstates $|\varepsilon\rangle$ to increasing $|V|$. We obtain $|\varepsilon\rangle$ by exact diagonalization and measure the scaled energies $\varepsilon_K = E_K/V = -(t/V)\langle \varepsilon | \sum_j \hat{a}_{j+1}^\dagger \hat{a}_j + h.c. | \varepsilon \rangle$ and $\varepsilon_V = E_V/V = \langle \varepsilon | \hat{l} | \varepsilon \rangle$, where E_K and E_V are the kinetic energy and interaction energy, respectively. The total energy is thus $\varepsilon = \varepsilon_K + \varepsilon_V$. Without loss of generality, we always choose $V > 0$ [46]. The first observation is a distinct collective behavior of eigenstates as V increases, where $|\varepsilon\rangle$, sorted in order of ε , spontaneously reorganize themselves such that interaction energies ε_V aggregate from a continuum (Fig. 1a) to a configuration of discrete plateaus (Fig. 1b). Each plateau is associated with an integer in $0, 1, \dots, N - 1$ which approximates ε_V , meaning that the eigenstates constructing a plateau are spanned mostly by Fock bases with the same number of NN links. Common structures that classify eigenstates are identified by the coexistent splitting of $\langle \varepsilon | \hat{s} | \varepsilon \rangle$ (SI).

An immediate question is how the gaps in ε_V open as V increases. To address finite-size effects, we estimate the i^{th} gap Δ_i (where $i = 1$ to $N - 1$, counting from left to right in Fig. 1b) between two adjacent plateaus

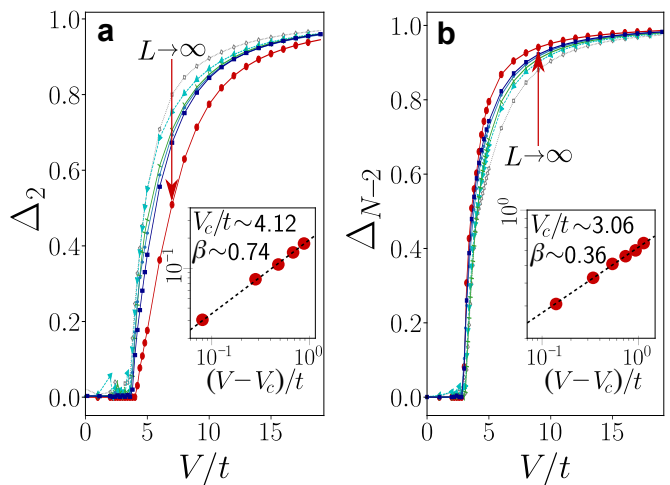


FIG. 2: Extrapolations of plateau gaps. Gaps Δ_i versus V/t for various system sizes ($L = 10, 12, \dots, 18$, along the arrow direction). The red solid dots represent the extrapolation to $L \rightarrow \infty$, resulting in (a) $V_c/t \sim 4.12$ for Δ_2 , and (b) $V_c/t \sim 3.06$ for Δ_{N-2} . Insets: Δ_i versus $(V - V_c)/t$ on logarithmic scales, confirming the power law relationship (dashed lines) with exponents $\beta_2 \sim 0.74(2)$ and $\beta_{N-2} \sim 0.36(1)$.

by extrapolating $L \rightarrow \infty$. Figure 2 shows examples of Δ_2 and Δ_{N-2} as functions of V/t (SI). Remarkably, the gaps behave similarly to order parameters in equilibrium critical phenomena that present continuous phase transitions: with a critical interaction strength V_c , the gap Δ_i is zero in the subcritical regime ($V < V_c$) and continuously increases to a nonzero value in the supercritical regime ($V > V_c$). Drawing an analogy with phase transitions, we examine the existence of universal power laws $\Delta_i \propto (V - V_c)^{\beta_i}$ as $(V - V_c) \rightarrow 0^+$, where β_i is the critical exponent for the i^{th} gap. The insets in Fig. 2 show a great agreement with the power-law behavior, where fits to logarithmic scales (dashed lines) measure the values of β_2 and β_{N-2} with impressive precision. Estimations reveal different values for each gap, with β_i ranging from $\beta_1 \approx 1$ to $\beta_{N-1} \approx 0$ (SI), indicating a distinct universal pattern associated with the common structures during the formation of plateaus.

Theoretical framework.— To analyze the eigenstates in the presence of common structures and plateaus, we consider strong interactions and employ a perturbative treatment of (t/V) . This approach renders the zeroth-order Hamiltonian as \hat{l} augmented by the singlon motions conserving \hat{l} , where the zeroth-order interaction energy, denoted as $l_0 = 0, 1, \dots, N-1$, dominates the plateaus. As detailed in the SI, higher-order processes systematically restore l_0 , outweighing its detrimental effects in the thermodynamic limit. Consequently, ε_V aggregates around l_0 and forms plateaus. Existing plateaus directly lead to the high-mobility states on either side. Since the interaction energies within a plateau closely approximate l_0 , the states on either side with the highest or lowest total energy exhibit extreme kinetic energies. As a result, peaks of $|\varepsilon_K|$, indicative of high mobility, appear on both sides of a given plateau, as illustrated in Fig. 1b.

Extreme value statistics. The quantum nature of the model allows a wavefunction to seep from its zeroth-order space, leading to a nonequivalence between ε_V and l_0 , thereby widening the plateaus (Fig. 1b). Treating this as an indicator of the emergence of plateaus, we compute the leakage $W(\varepsilon) = \sum_{f'} |\langle f' | \varepsilon \rangle|^2$ with all Fock bases $|f'\rangle$ satisfying $\langle f' | \hat{l} | f' \rangle \neq l_0$, and analyze the probability distribution $P(W)$ to fully describe all eigenstates. Figs. 3a and 3b illustrate that $P(W)$ transitions from a symmetric form to a distorted one as V surpasses t and reaches a value where the interaction energy dominates the entire spectrum ($\varepsilon_V^{\max} - \varepsilon_V^{\min} > \varepsilon_K^{\max} - \varepsilon_K^{\min}$).

Our argument suggests that $P(W)$ undergoes a transition from a normal distribution to a form described by extreme value statistics. For the probability distribution of an eigenstate, $P_\varepsilon(f) = |\langle f | \varepsilon \rangle|^2$, the leakage weight $W(\varepsilon) = \sum_{f'} P_\varepsilon(f')$ simulates the mean of the samples at f' , where $\langle f' | \hat{l} | f' \rangle = l'_0 \neq l_0$. For a weaker interaction,

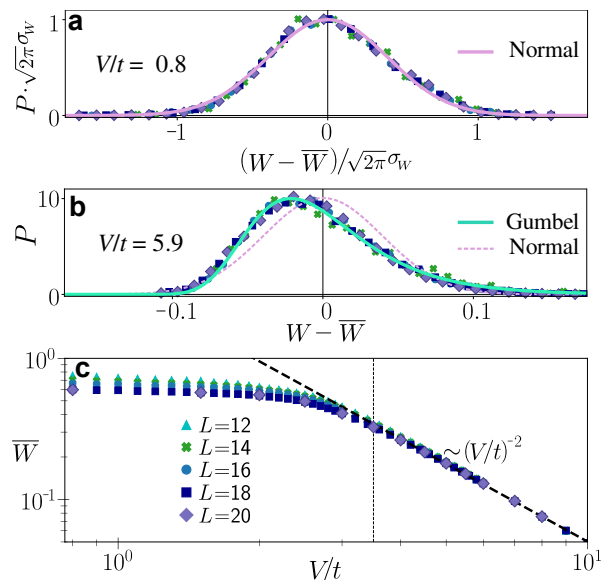


FIG. 3: Emergent extreme value statistics. The weight $W(\varepsilon)$ is obtained for all eigenstates $|\varepsilon\rangle$ with various L , the statistics are performed in the middle of the spectrum. (a) and (b) depict the probability distribution $P(W)$ for $V/t = 0.8$ and 5.9 respectively, with the mean value \bar{W} and the standard deviation σ_W . Solid lines show the best fit to the data, where the Gumbel distribution is $P(x) = \frac{1}{\sigma_W} \exp[-(x + e^{-x})]$ with $x = (W - \bar{W})/\sigma_W$ and $\sigma_W = 0.038(2)$. The dashed line in (b) is a normal-distribution fit for comparison; the displacement between the peaks of the two fittings is $\sim 0.58(3)\sigma_W$. (c) \bar{W} versus V/t , indicating a decrease $\propto (t/V)^2$ for $V/t \gtrsim 3.5$, data for different L collapse after a slight vertical shift.

eigenstates naturally spread across all bases, thereby P_ε remains qualitatively the same, and the $P_\varepsilon(f')$ act as random samples returning arbitrary values in P_ε . According to the central limit theorem, the distribution of the mean of random samples, i.e., $P(W)$, converges to a normal distribution as shown by Fig. 3a. However, for a large interaction causing wavefunctions to concentrate in the zeroth-order space, the leakage decreases. $P_\varepsilon(f')$ no longer presents random samples in P_ε ; instead, it goes to vanishingly small values as the interaction increases. The statistics of $P_\varepsilon(f')$ in such a scenario naturally lead to the statistics of minimums, described by the generalized extreme value theory [37]. Assuming that decreased leakages cause $P_\varepsilon(f')$ to decay exponentially as l'_0 moves away from l_0 , then $P(W)$ is predicted to be governed by the Gumbel distribution. Fig. 3b demonstrates good consistency between this distribution and our dataset.

Moreover, $W(\varepsilon)$ can be estimated as $(\frac{t}{V})^2 |\langle \varepsilon_1 | \varepsilon_1 \rangle|^2$, the decrease in leakage is then expected to be proportional to $(V/t)^{-2}$. Fig. 3c illustrates the mean value $\bar{W} = \frac{1}{\Omega} \sum_\varepsilon W(\varepsilon)$ versus V/t . The decrease is observed around $V/t \sim 3.5$, indicating where ε_V begins to aggregate into plateaus and common structures start to emerge in eigenstates. This observation aligns with

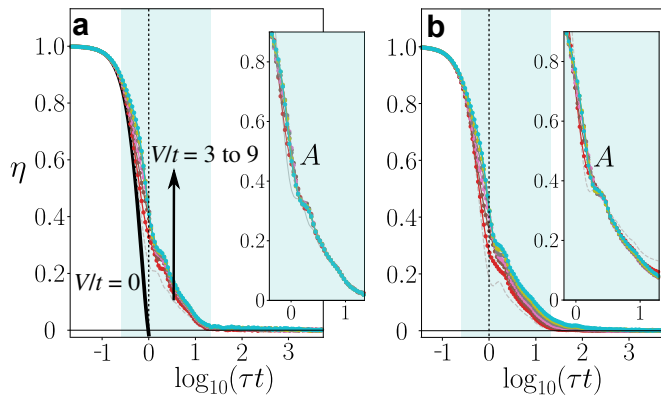


FIG. 4: Equilibration of Fock states. (a) $\eta(\tau)$ for $L = 18$, two stages of dynamics are observed before and after $\tau t \sim 1$. The inset shows the universal form $A(\tau)$ with $\epsilon \sim 0.05$ (see the main text), which governs the dynamics in the presence of eigenstate common structures. (b) Similar to (a) but with dipole-dipole interactions $V_{i,j} = V/|i-j|^3$ and $\epsilon \sim 0.25$, the universal function $A(\tau)$ is almost unchanged.

the analytical estimation in the SI. Comparing with the V_c/t in Fig. 2, it becomes evident that along with the emergence of common structures, most ϵ_V aggregate around l_0 even before gaps open. The latter stringently requires the two states with exactly the highest and lowest ϵ_V in two adjacent plateaus.

Universal dynamics.— The diminishing leakage of wavefunctions from their zeroth-order spaces implies a reduction in the traversed area within Hilbert space during time evolution. As detailed in the SI, the evolution of Fock states conserve \hat{l} to the first order of (t/V) while allowing \hat{s} to change. The dynamics are therefore grounded by the initial number of NN links to a great degree.

To align with experiments, we investigate this impact by examining the equilibration of Fock states $|f_0\rangle$ with the j_0^{th} site initially occupied. We compute $\eta(\tau) = [\langle f_0(\tau) | \hat{n}_{j_0} | f_0(\tau) \rangle - N/L] / (1 - N/L)$, where $\eta = 1$ indicates that the initially observed particle is localized at j_0 , while $\eta = 0$ implies that it has dissipated into the background. Assuming that the initial preparation [38–40] does not favor particular configurations, we average $\eta(\tau)$ over all $|f_0\rangle$ for a statistical description. The dynamics depicted in Fig. 4a unveil two stages. For $\tau t \lesssim 1$, free-moving singlons dominate the dynamics, yet the final equilibration at $\eta = 0$ is not achieved, contrasting with the behavior of free-moving particles with $V = 0$. This suggests that singlons alone do not furnish sufficient motion to connect $|f_0\rangle$ equally to j_0 -occupied and j_0 -empty states. Nonetheless, equilibration persists. For $\tau t \gtrsim 1$, the spread of singlons saturates, uncovering the remaining higher-order processes. These processes compel equilibration to progress until $\eta = 0$.

The slight variations associated with different values of V/t reflect the interaction dependence of the higher-order

processes. The approximation to the first order allows us to express $\eta(\tau) \sim A(\tau) - B(\tau) \cdot t/V$, with $A(\tau)$ and $B(\tau)$ being V -independent functions representing dynamics concerning NN links (SI). Assuming $B(\tau) \sim A(\tau) + \epsilon$ for simplicity, the dynamics can be described by a universal form $A(\tau) \sim [\eta(\tau) + \frac{\epsilon}{V}]/(1 - \frac{\epsilon}{V})$ (Fig. 4a).

Conclusions.— We have studied a generic 1D quantum lattice model and uncovered a profound relationship between out-of-equilibrium dynamics and emergent properties in eigenstates across the spectrum. Specifically, a strong yet finite inter-site interaction induced inherent structures within the eigenstates, leading to the reorganization of wavefunctions across the Fock bases and the opening of gaps in interaction energy akin to continuous phase transitions. These structured eigenstates exhibit statistical patterns described by extreme value theory and compress the area of time evolution, wherein the equilibration of Fock states unfolds through multiple stages with a universal nature.

Our findings, particularly regarding the dynamical aspects, demonstrate significant consistency across a broad range of realistic interactions (e.g., Fig. 4b), suggesting that our observations are not consequences of the non-thermal feature originating from the NN interacting form [41]. This offers a comprehensive understanding of recent observations [23], wherein a qualitative slowdown of quench expansion is confirmed with interaction strengths close to those associated with eigenstate structures.

The EHM under examination is isomorphic to the XXZ model, where the structured eigenstates provide deeper insight into the transformation of the self-return probability [34] observed previously. Earlier studies have revealed far-from-equilibrium spin transport in the XXZ model, elucidated by near-equilibrium theory [35, 36]. However, this behavior relies on initial conditions embodying a certain equilibrium background. In contrast, initial Fock states circumvent such limitations, focusing on the essence of dynamics far from equilibrium. The reduced evolving area of Fock states presents weakened ergodicity due to interactions, a phenomenon that should be distinguished from non-thermal states arising from kinetic constraints [42, 43].

Acknowledgements.— The authors express their gratitude for the insightful discussions with Roderich Moessner and appreciate his constructive comments throughout the completion of this project.

* Electronic address: weihan@pks.mpg.de

† Electronic address: ab.saberi@ut.ac.ir, saberi@pks.mpg.de

- [1] J. Eisert, M. Friesdorf, and C. Gogolin, Nat. Phys. 11, 124 (2015).
- [2] C. Gogolin and J. Eisert, Rep. Prog. Phys. 79 056001 (2016).

- [3] I. Bloch, J. Dalibard, and W. Zwerger, *Rev. Mod. Phys.* 80, 885 (2008); J. Dalibard and S. Nascimbène, *Nature Phys.* 8, 267 (2012).
- [4] T. Langen, R. Geiger, and J. Schmiedmayer, *Annu. Rev. Condens. Matter Phys.* 6, 201 (2015).
- [5] C. Gross, and I. Bloch, *Science* 357, 995. (2017).
- [6] T. Stöferle, H. Moritz, C. Schori, M. Köhl, and T. Esslinger, *Phys. Rev. Lett.* 92, 130403 (2004); M. Köhl, H. Moritz, T. Stöferle, C. Schori, and T. Esslinger, *J. Low Temp. Phys.* 138, 635–644 (2005).
- [7] M. Greiner, O. Mandel, T. Esslinger, T. Hänsch and I. Bloch, *Nature* 415, 39 (2002).
- [8] I. B. Spielman, W. D. Phillips, and J. V. Porto, *Phys. Rev. Lett.* 98, 080404 (2007).
- [9] T. Esslinger, *Annu. Rev. Condens. Mat. Phys.* 1, 129 (2010).
- [10] U. Schneider, L. Hackermüller, J. P. Ronzheimer, S. Will, S. Braun, T. Best, I. Bloch, E. Demler, S. Mandt, D. Rasch, and A. Rosch, *Nature Phys.* 8, 213 (2012).
- [11] S. Trotzky, Y.-A. Chen, A. Flesch, I. P. McCulloch, U. Schollwöck, J. Eisert, and I. Bloch, *Nat. Phys.* 8, 325 (2012).
- [12] J. P. Ronzheimer, M. Schreiber, S. Braun, S. S. Hodgman, S. Langer, I. P. McCulloch, F. Heidrich-Meisner, I. Bloch, and U. Schneider, *Phys. Rev. Lett.* 110, 205301 (2013).
- [13] L. Xia, L. A. Zundel, J. Carrasquilla, A. Reinhard, J. M. Wilson, M. Rigol, and D. S. Weiss, *Nat. Phys.* 11, 316 (2015).
- [14] S. Scherg, T. Kohlert, J. Herbrych, J. Stolpp, P. Bordia, U. Schneider, F. Heidrich-Meisner, I. Bloch, and M. Aidelsburger, *Phys. Rev. Lett.* 121, 130402 (2018).
- [15] S. Hild, T. Fukuhara, P. Schauß, J. Zeiher, M. Knap, E. Demler, I. Bloch, and C. Gross, *Phys. Rev. Lett.* 113, 147205 (2014).
- [16] P. N. Jepsen, J. Amato-Grill, I. Dimitrova, W. W. Ho, E. Demler, and W. Ketterle, *Nature* 588, 403 (2020).
- [17] N. Defenu, T. Donner, T. Macrì, G. Pagano, S. Ruffo, and A. Trombettoni, *Rev. Mod. Phys.* 95, 035002 (2023).
- [18] A. de Paz, A. Sharma, A. Chotia, E. Maréchal, J. H. Huckans, P. Pedri, L. Santos, O. Gorceix, L. Vernac, and B. Laburthe-Tolra, *Phys. Rev. Lett.* 111, 185305 (2013).
- [19] A. Patscheider, B. Zhu, L. Chomaz, D. Petter, S. Baier, A.-M. Rey, F. Ferlaino, and M. J. Mark, *Phys. Rev. Research* 2, 023050 (2020).
- [20] P. Scholl, M. Schuler, H. J. Williams, A. A. Eberharter, D. Barredo, K.-N. Schymik, V. Lienhard, L.-P. Henry, T. C. Lang, T. Lahaye, A. M. Läuchli, and A. Browaeys, *Nature (London)* 595, 233 (2021).
- [21] S. Baier, M. J. Mark, D. Petter, K. Aikawa, L. Chomaz, Z. Cai, M. Baranov, P. Zoller, and F. Ferlaino, *Science* 352, 201 (2016).
- [22] L. Su, A. Douglas, M. Szurek, R. Groth, S. F. Ozturk, A. Krahn, A. H. Hébert, G. A. Phelps, S. Ebadi, S. Dickerson, F. Ferlaino, O. Marković, and M Greiner, *Nature* 622, 724–729 (2023).
- [23] E. Guardado-Sanchez, B. M. Spar, P. Schauss, R. Belyansky, J. T. Young, P. Bienias, A. V. Gorshkov, T. Iadecola, and W. S. Bakr, *Phys. Rev. X* 11, 021036 (2021).
- [24] E. G. Dalla Torre, E. Berg, and E. Altman, *Phys. Rev. Lett.* 97, 260401 (2006).
- [25] Xiaolong Deng and Luis Santos, *Phys. Rev. B* 84, 085138 (2011).
- [26] T. Lahaye, C. Menotti, L. Santos, M. Lewenstein and T. Pfau, *Rep. Prog. Phys.* 72 126401 (2009).
- [27] O. Dutta, M. Gajda, P. Hauke, M. Lewenstein, D.-S. Lühmann, B. A. Malomed, T. Sowiński and J. Zakrzewski, *Rep. Prog. Phys.* 78 066001 (2015).
- [28] L. Barbiero, C. Menotti, A. Recati, and L. Santos, *Phys. Rev. B* 92, 180406(R) (2015).
- [29] W.-H. Li, A. Dhar, X. Deng, K. Kasamatsu, L. Barbiero, and L. Santos, *Phys. Rev. Lett.* 124, 010404 (2020).
- [30] W.-H. Li, A. Dhar, X. Deng, and L. Santos, *Phys. Rev. A* 103, 043331 (2021).
- [31] W.-H. Li, X. Deng, and L. Santos, *Phys. Rev. Lett.* 127, 260601 (2021).
- [32] H. Korbmayer, P. Sierant, W. Li, X. Deng, J. Zakrzewski, and L. Santos, *Phys. Rev. A* 107, 013301 (2023).
- [33] P. Nozières, *J. Low Temp. Phys.* 137, 45–67 (2004).
- [34] G. Misguich, V. Pasquier, and J.-M. Kuck, *Phys. Rev. B* 94, 155110 (2016).
- [35] R. Steinigeweg, F. Jin, D. Schmidtke, H. De Raedt, K. Michielsen, and J. Gemmer, *Phys. Rev. B* 95, 035155 (2017).
- [36] M. Ljubotina, M. Žnidarič, and T. Prosen, *Nat. Commun.* 6, 16117 (2017).
- [37] S. N. Majumdar, A. Pal, and G. Schehr, *Physics Reports*, 840, pp.1-32 (2020).
- [38] W. S. Bakr, J. I. Gillen, A. Peng, S. Fölling, and M. Greiner, *Nature* 462, 74 (2009).
- [39] S. Kuhr, *Natl. Sci. Rev.*, 3, 170 (2016).
- [40] C. Gross and W. Bakr, *Nat. Phys.* 17, 1316 (2021).
- [41] Bill Sutherland (2004), *Beautiful Models: 70 Years of Exactly Solved Quantum Many-Body Problems*
- [42] M. Serbyn, D.A. Abanin, and Z. Papić, *Nat. Phys.* 17, 675–685 (2021).
- [43] V. Khemani, M. Hermele, and R. Nandkishore, *Phys. Rev. B* 101, 174204 (2020).
- [44] Eq. (1) is also called the t - V model, it describes a hardcore Bose lattice gas, which can be mapped into the XXZ model by Holstein–Primakoff transformation, so, half-filling is associated with zero magnetization. In 1D, the XXZ model can be again mapped into a spinless Fermi lattice gas by Jordan–Wigner transformation.
- [45] Besides singlons’ connection, a common structure is also shared between translating or reflecting counterparts of Fock bases due to the symmetry of Eq. (1). But this does not affect our concern in this work.
- [46] For the XXZ model [44], consider $\mathcal{U} = \exp(i\pi \sum_j j \hat{S}_j^z)$, a rotation by π about z -axis for every second spin, where $\hat{S}^z = \frac{1}{2} \hat{\sigma}^z$. The unitary transform $\mathcal{U}^\dagger H(V) \mathcal{U} = -H(-V)$ gives the spectrum relationship $E(-V) = -E(V)$. So $E(-V)$ and $E(V)$ are exact reflections of each other to $E = 0$, note that the ground state for $-V$ corresponds to the highest excited state for V . Hence, to investigate $E(V)$ with a varying $|V|$, taking $V > 0$ will be enough.

Supplementary Information for: Eigenstate plateau transition and equilibration in 1D quantum lattice models

Wei-Han Li^{1,*} and Abbas Ali Saberi^{2,1,†}

¹Max Planck Institute for the Physics of Complex Systems, 01187 Dresden, Germany

²Department of Physics, University of Tehran, P. O. Box 14395-547, Tehran, Iran

This Supplementary Information begins with details for common structures and plateau transitions (Sec. I). It is followed by the perturbation analysis (Sec. II) that predicts the plateaus as well as the required interactions (Sec. III), and ends with the dynamical results (Sec. IV).

I. DETAILS FOR PLATEAU TRANSITION

As discussed in the main text, an increasing V leads to coexist response parameters in an eigenstate $|\varepsilon\rangle$, the

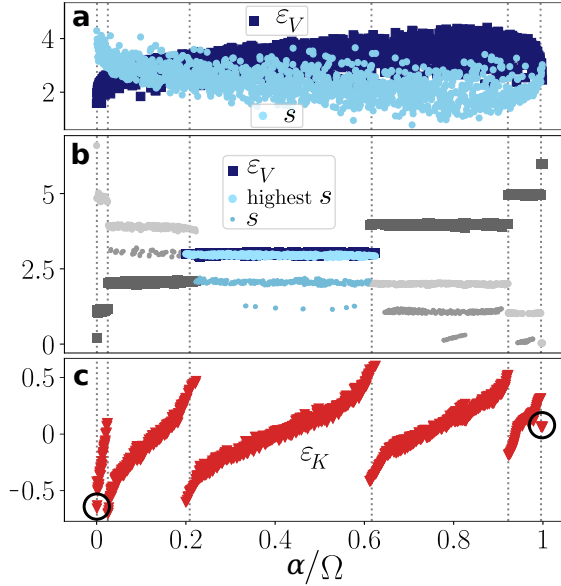


FIG. S1: Details of emergent plateaus. The scaled interaction energy ε_V (dark \blacksquare), expected singlon number s (light \bullet), and scaled kinetic energy ε_K (red \blacktriangledown) for the eigenstates labeled by $\alpha = 1, \dots, \Omega$ sorted in ascending order of total energy $\varepsilon = \varepsilon_V + \varepsilon_K$. Where Ω is the dimension of the Hilbert space for $N/L = 7/14$. (a) ε_V and s for $V/t = 1$. (b) ε_V and s for $V/t = 8$, eigenstates exhibit a common structure when their ε_V falls within the same plateau, and s is at the same level. Note that s is at its maximum level at the two sides of each plateau. (c) ε_K for $V/t = 8$; bandwidths extend in the middle of the total energy spectrum but approach zero at the edges (solid circles).

scaled interaction energy $\varepsilon_V(\varepsilon) = \langle \varepsilon | \hat{I} | \varepsilon \rangle$ and the number of singlons $s(\varepsilon) = \langle \varepsilon | \hat{s} | \varepsilon \rangle$. As demonstrated in Figs. S1a and S1b, discrete levels of s accompany the formation of plateaus. Eigenstates belong to the same plateau of ε_V and the same level of s share a common structure. Note that states belonging to different common structures can not have the same ε_V but may have the same s . Within a plateau, states existing at the two sides consistently exhibit the highest singlon count (Fig. S1b) as well as the extreme values of kinetic energy ε_K (Fig. S1c). This observation confirms the high-mobility states shown by $|\varepsilon_K|$ discussed in the main text. At the edges of the total energy spectrum, ε_V characterizes the total energy as the bandwidth of ε_K diminishes (Fig. S1c, circles), however, ε_K diverges in the middle of the spectrum, leaving the spectrum continuous as shown in the main text. We shall return to this in Sec. II.

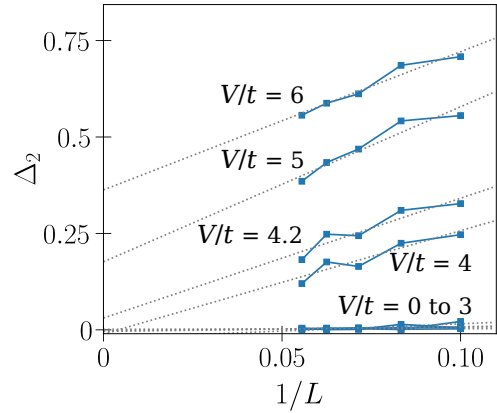


FIG. S2: The extrapolation. Concerning finite-size effects, the gap values are estimated for various V/t by stretching Δ_i as a function of $1/L$. The figure shows data for Δ_2 .

To investigate the critical behavior of gaps Δ_i opening in the continuum of ε_V , we extrapolate Δ_i as a function of $1/L$ (e.g., Fig. S2) and examine the power-law scaling $\Delta_i \propto (V - V_c)^{\beta_i}$ in the vicinity of $(V - V_c) \rightarrow 0^+$. Fig. S3 depicts the extrapolated gaps against the interaction, the insets illustrate the opening gaps in agreement with the power-law scaling. The exponents β_i vary across different gaps, indicating that the detailed mechanisms involved in the plateau formations are associated with the common structures. Approaching the middle of the spectrum, larger system sizes are necessary to ensure numerical convergence for the extrapolation, the values of V_c and β_i estimated in this situation may have larger errors (e.g., Fig. S3e).

*Electronic address: weihan@pks.mpg.de

†Electronic address: ab.saberi@ut.ac.ir, saberi@pks.mpg.de

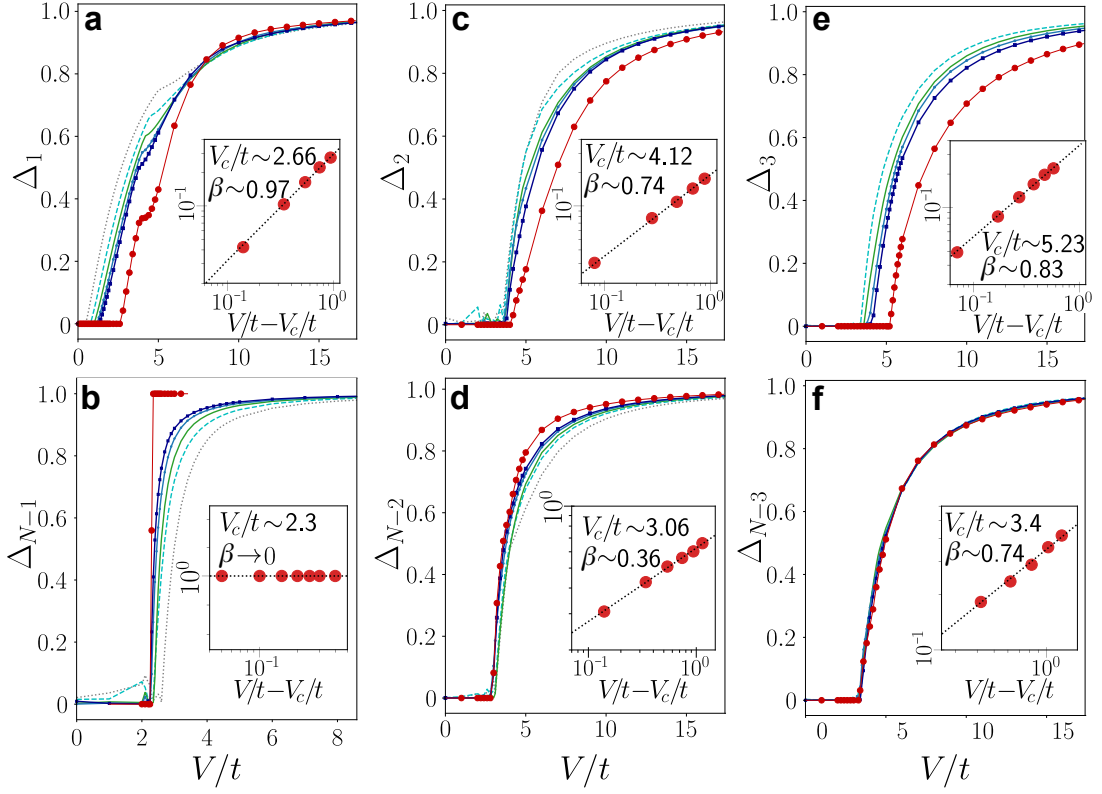


FIG. S3: Extrapolations of plateau gaps. Gap Δ_i versus V/t for $i = 1, 2, \dots, N-1$. The red solid dots represent extrapolations to the $1/L \rightarrow 0$. Insets show the V_c/t and β_i determined by examining the power-law scaling relationship $\Delta_i \propto (V/t - V_c/t)^{\beta_i}$ in the vicinity of $(V/t - V_c/t) \rightarrow 0^+$. Panels (a)-(d) display gaps near the edges of the spectrum, with system sizes $L = 10, 12, \dots, 18$. Panels (e) and (f) depict gaps situated deeper in the spectrum with $L = 12$ to 18 .

II. PERTURBATION TREATMENTS

For the EHM in the main text, we consider large interactions and treat (t/V) perturbatively. This leaves $H/V = \hat{l} - (t/V)\hat{K}$. Where $\hat{K} = \sum_j (\hat{a}_{j+1}^\dagger \hat{a}_j + \hat{a}_j^\dagger \hat{a}_{j+1})$ includes all the hopping, and the number of NN links $\hat{l} = \sum_j \hat{n}_{j+1} \hat{n}_j$ is our unperturbed Hamiltonian diagonalized by Fock bases $|f\rangle$. The term \hat{l} degenerates extensively as $\langle f|\hat{l}|f\rangle = l_0 = 0, 1, \dots, N-1$ is strongly limited. We thus combine \hat{l} with the part of the hopping terms conserving NN links. The model Hamiltonian then becomes

$$H/V = \tilde{H}_0 - (t/V)\tilde{K}. \quad (\text{S1})$$

The term \tilde{H} governs the transition between Fock bases possessing the same l_0 —representing the singlon motions discussed above, while \tilde{K} describes the transition between states with l_0 and $l_0 \pm 1$.

Let $\{l_0\}$ be the subspace spanned by $|f\rangle$ with $\langle f|\hat{l}|f\rangle = l_0$, then \tilde{H} is represented as $\tilde{H}_0 \oplus \tilde{H}_1 \oplus \dots \oplus \tilde{H}_{l_0} \dots \tilde{H}_{N-1}$. The sub-Hamiltonian \tilde{H}_{l_0} has identical diagonal terms l_0 and off-diagonal terms $-(t/V)$ describing the amplitude of singlon hopping. The singlon motions conserve l_0 , in other words, they are not allowed to be adjacent, either to each other or to other particles. This means

singlons live in reduced lattices

$$L_s = L - N + l_0 < L. \quad (\text{S2})$$

The total number of singlons is constrained, it is related to the number of NN links by

$$N = \hat{l} + \hat{s} + \hat{c}, \quad (\text{S3})$$

where \hat{c} represents the number of clusters. A cluster is defined as an array of particles with no holes between them, or, a particle configuration that can be connected to such an array via singlon motions.

For an arbitrary basis $|f\rangle$, we denote the number of NN links, singlons, and clusters respectively by

$$\langle f|\hat{l}|f\rangle = l_0, \quad \langle f|\hat{s}|f\rangle = N_s, \quad \text{and} \quad \langle f|\hat{c}|f\rangle = N_c. \quad (\text{S4})$$

Where $l_0 = 0, 1, \dots, N-1$, for a given l_0 , $N_c = 0$ if $l_0 = 0$, otherwise $N_c = 1, 2, \dots, \min(l_0, N - l_0)$, and $N_s = N - l_0 - N_c$ (Eq. (S3)). It is clear that if $l_0 = 2, 3, \dots, N-2$, N_c and N_s are not unique, implying sub-blocks within \tilde{H}_{l_0} , although it does not affect the subsequent analysis.

A. Sub-Hamiltonians and the zeroth-order energy

The sub-Hamiltonian \tilde{H}_{l_0} is equivalent to the EHM in the main text with N_s particles, L_s sites, and $V = 0$,

which can be mapped into the XX model with magnetization $L_s - 2N_s$ and zero transverse fields. The eigenvalues are given [1] as

$$\varepsilon_{0,a} = l_0 + (t/V)\Lambda_a, \text{ with } \Lambda_a = -2 \sum_{j=1}^{N_s} \cos\left(\frac{2\pi m_j}{L_s}\right), \quad (\text{S5})$$

where $l_0 = \varepsilon_{V0}$ and $(t/V)\Lambda_a = \varepsilon_{K0}$ are the zeroth orders of ε_V and ε_K respectively.

The lower index a labels a total of $\binom{L_s}{N_s}$ states in \tilde{H}_{l_0} , and the number m_j are non-repeating integers selected from the range $[0, L-1]$ for fermions or an odd number of bosons, but half-integers selected from $[\frac{1}{2}, L - \frac{1}{2}]$ for an even number of bosons. Choosing $m_j = 0, \dots, N_s - 1$ for the former case gives the lowest energy of Eq. (S5),

$$-\Lambda_{min} = 2 \cos\left[\frac{\pi(N_s - 1)}{L_s}\right] \frac{\sin(\pi N_s/L_s)}{\sin(\pi/L_s)}. \quad (\text{S6})$$

Note that choosing $m_j = \frac{1}{2}, \dots, N_s - \frac{1}{2}$ for the later case lead to the same result at $L_s \rightarrow \infty$.

The bandwidth for eigenstates of \tilde{H}_{l_0} is $\Delta\varepsilon_0 = \Delta\varepsilon_{K0} = (t/V)(\Lambda_{max} - \Lambda_{min}) = (2t/V)|\Lambda_{min}|$. Within a plateau, where ε_V approaches l_0 thus $\Delta\varepsilon$ is close to $\Delta\varepsilon_K \sim \Delta\varepsilon_{K0} \propto |\Lambda_{min}|$. At the left and right edges of the total energy spectrum, the involved Fock bases are the kinds of $|\bullet \circ \bullet \circ \bullet \circ \bullet \circ\rangle$ and $|\bullet \circ \bullet \circ \bullet \circ \bullet \circ \circ \bullet \circ\rangle$ respectively, the value of N_s is either L_s or 0, therefore $\Delta\varepsilon_K \rightarrow 0$. While in the middle of the spectrum, $\Delta\varepsilon_K \propto \frac{1}{\sin(\pi/L_s)}$ diverges at the thermodynamic limit, hence the total energy $\varepsilon = \varepsilon_V + \varepsilon_K$ forms a continuum despite the gaps in ε_V . The numerical results of $\Delta\varepsilon_K$ shown in Fig. S1c confirm this deriving.

B. Eigenvectors and recovering processes

In the following, we omit the lower index a of the zeroth-order $\varepsilon_{0,a}$, and expand the eigenstates by the perturbation formulation [2, 3]

$$|\varepsilon\rangle = |\varepsilon_0\rangle + \sum_{k=1}^{\infty} (t/V)^k |\varepsilon_k\rangle. \quad (\text{S7})$$

Where $|\varepsilon_0\rangle$ lives in $\{l_0\}$, the space of \tilde{H}_{l_0} , is the zeroth-order state corresponds to ε_0 , $|\varepsilon_k\rangle$ is the term involving virtual processes that consist of k times of actions of \tilde{K} . As illustrated in Fig. S4, these actions bring $|\varepsilon_0\rangle$ away from $\{l_0\}$ via transfers between adjacent subspaces. The first term reads

$$|\varepsilon_1\rangle = \sum_{|\varepsilon'_0\rangle \in \{l'_0\}} \frac{\langle \varepsilon'_0 | \tilde{K} | \varepsilon_0 \rangle}{\varepsilon_0 - \varepsilon'_0} \cdot |\varepsilon'_0\rangle, \quad (\text{S8})$$

where $\{l'_0\} = \{l_0 \pm 1\}$. As illustrated in Fig. S4a (left), $|\varepsilon_1\rangle$ estimates those components of $|\varepsilon\rangle$ possessing $l_0 \pm 1$ NN links, it gives the leading contribution to the leakage $W(\varepsilon)$ discussed in the main text.

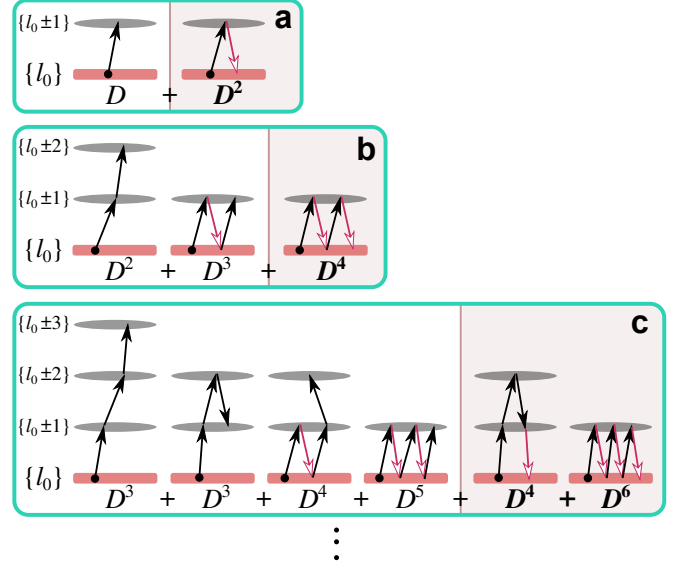


FIG. S4: Perturbation processes originate from \tilde{K} . A process is a sequence of actions of \tilde{K} , through which the zeroth-order state (black dots) is brought away from its subspace $\{l_0\}$ and transferred between adjacent subspaces. For a given process, the order of (t/V) is the number of transfers (arrows) except for those transferring from $\{l_0 \pm 1\}$ back to $\{l_0\}$ (red arrows). The processes recovering l_0 are shown in the shaded areas. Powers of $D \propto L^2$ estimate the number of pathways for each process, a polynomial of D is thus left for each order of (t/V) . The panel (a), (b) and (c) show processes in the 1-st, 2-nd, and 3-rd order of (t/V) respectively.

The second term is

$$|\varepsilon_2\rangle = \sum_{\substack{|\varepsilon''_0\rangle \in \{l''_0\} \\ \varepsilon''_0 \neq \varepsilon_0}} \sum_{|\varepsilon'_0\rangle \in \{l'_0\}} \frac{\langle \varepsilon''_0 | \tilde{K} | \varepsilon'_0 \rangle \langle \varepsilon'_0 | \tilde{K} | \varepsilon_0 \rangle}{(\varepsilon_0 - \varepsilon''_0)(\varepsilon_0 - \varepsilon'_0)} \cdot |\varepsilon''_0\rangle. \quad (\text{S9})$$

It involves two actions of \tilde{K} , bring $|\varepsilon_0\rangle$ intermediately to $|\varepsilon'_0\rangle \in \{l'_0\} = \{l_0 \pm 1\}$ and then to $|\varepsilon''_0\rangle \in \{l''_0\} = \{l'_0 \pm 1\}$. Crucially, $|\varepsilon_0\rangle$ is brought back to $\{l_0\}$ when $\{l''_0\} = \{l_0\}$, which leaves $(t/V)^2 |\varepsilon_2\rangle \sim \mathcal{O}(t/V)$ not $\mathcal{O}(t^2/V^2)$. As the denominator $(\varepsilon^0 - \varepsilon''^0) \propto (t/V)$ when both ε^0 and ε''^0 are eigenvalues of the same \tilde{H}_{l_0} (Eq. (S5)), thereby one factor of (t/V) is reduced. This kind of process (Fig. S4a right) enables the connections between states with the same NN links but different singlons.

The higher-order terms of Eq. (S7) are constructed systematically through the expansion formulation [2, 3], Figs. S4b and S4c illustrate few of them. Remarkably, a transfer that brings a state in $\{l_0 \pm 1\}$ back to $\{l_0\}$ always reduces one factor of (t/V) by the involved denominator—a difference between two eigenvalues of the same \tilde{H}_{l_0} (Eq. (S5)). A term $(t/V)^k |\varepsilon_k\rangle$ of the expansion Eq. (S7) is thus in the order of $(t/V)^{k-k'}$ if $|\varepsilon_k\rangle$ contains k' times of $\{l_0 \pm 1\} \rightarrow \{l_0\}$ transfers. Red arrows in Fig. S4 show transfers of this kind.

III. PLATEAU STABILITY AT THE THERMODYNAMIC LIMIT

Processes bringing $|\varepsilon_0\rangle$ back to $\{l_0\}$ shown in Fig. S4 (shaded areas) can lead to aggregation of the interaction energy ε_V to its zeroth-order approximation $\varepsilon_{V0} = l_0$. Here we argue that the responsible mechanism holds at the thermodynamic limit $L \rightarrow \infty$.

The leading departure of $|\varepsilon_0\rangle$ from $\{l_0\}$ originates from $(t/V)|\varepsilon_1\rangle \sim \mathcal{O}(t/V)$ (Fig. S4a left), which introduces a factor D , quantifying the number of pathways through \tilde{K} that create or annihilate a NN link in $|\varepsilon_0\rangle$. Thereby, D scales proportionally to the number of singlons and clusters, i.e., $D \propto \langle \varepsilon_0 | \hat{s} \hat{c} | \varepsilon_0 \rangle \sim \mathcal{O}(L^2)$. The divergence of D at the limit $L \rightarrow \infty$, however, does not negate the significance of l_0 due to those processes in $|\varepsilon_2\rangle$ that bring $|\varepsilon_0\rangle$ intermediately to $\{l_0 \pm 1\}$, and then back to $\{l_0\}$ (Fig. S4a right). Through the intermediate states, $|\varepsilon'_0\rangle$, the returning processes reduce one (t/V) as discussed in Sec. IIB and introduce an additional factor $D' \propto \langle \varepsilon'_0 | \hat{s} \hat{c} | \varepsilon'_0 \rangle$. Hence, $(t/V)^2 |\varepsilon_2\rangle \sim \mathcal{O}(t/V)$ and an overall quantity of the pathways $D \cdot D' \sim D^2$.

As shown in Figs. S4b and S4c (shaded areas), the returning processes appear systematically in the higher order formulations. For a given order of $(t/V)^m$, the quantity of pathways for all processes is approached by $(D^{2m} + a_{2m-2} D^{2m-2} \dots) + (a_{2m-1} D^{2m-1} \dots + a_m D^m)$, where the left and right polynomials refer to the returning and the departing processes respectively. The highest-degree term, D^{2m} , contributes exclusively to the returning processes, bringing $|\varepsilon_0\rangle$ back and forth between $\{l_0\}$ and $\{l_0 \pm 1\}$ for m times, we therefore argue that the departure processes are overwhelmed at $L \rightarrow \infty$. As a result, ε_V aggregates around l_0 and a plateau emerges.

Required interactions

The aggregation, $\varepsilon_V \sim l_0 = 0, 1 \dots N - 1$, tells that the interaction energy dominates the pattern of the total energy spectrum, precisely, ε_V is significantly larger than $\Delta \varepsilon_K$. To estimate the required V/t , we start with

$$l_0 > \Delta \varepsilon_{K0}, \quad (\text{S10})$$

where $\Delta \varepsilon_{K0}$ determined by Eq. (S6). Since $\Delta \varepsilon_{K0} \rightarrow 0$ at the edges of the spectrum, we shall focus on the middle of it, where $\Delta \varepsilon_{K0}$ diverges as $\frac{1}{\sin(\pi/L_s)}$.

For l_0 to significantly exceeds $\Delta \varepsilon_{K0}$, we demand $l_0 > (4t/V) \left| \frac{\sin(\pi N_s/L_s)}{\sin(\pi/L_s)} \right|$, which serves as a sufficient condition of the inequality (S10) capturing the divergence of $\Delta \varepsilon_{K0}$ in the middle of the spectrum. The scenario $l_0 = N/2$ dominates the half-filling lattices at the thermodynamic limit, since the size of $\{l_0\}$ reduces exponentially when

l_0 departs from $N/2$. Let $l_0 = N/2$ and $L_s = L - N + l_0 = 3N/2$ (Eq. (S2)), we have $V/t > \frac{4}{N/2} \left| \frac{\sin(2\pi N_s/3N)}{\sin(2\pi/3N)} \right|$. The bandwidths, determined by the extreme kinetic energies, naturally imply the largest number of singlons allowed in the plateau, i.e., $N_s = N - l_0 - 1$ (Eq. (S3) with $\hat{c} = 1$), this is confirmed in Fig. S1c. Substituting the N_s and taking the limit $N \rightarrow \infty$ we end up with $V/t \gtrsim 3.31$, agreeing well with the results in the main text. Moreover, the complete form of the inequality (S10) approaches $V/t > (2L_s/\pi l_0) |\sin(2\pi N_s/L_s)|$ for $L_s \gg 1$. Again, let $l_0 = N/2$ and $L_s = 3N/2$, we obtain $V/t > \frac{6}{\pi} |\sin(4\pi N_s/3N)|$. The sufficient condition leaves $V/t > 6/\pi \sim 1.91$, curiously close to the critical value $V/t = 2$ for the well-known ground-state phase transition in the XXZ model.

IV. THE DYNAMICS OF FOCK STATES

For an arbitrary Fock state $|f\rangle$, the time evolution is given by $\langle f' | f(\tau) \rangle = \sum_{\varepsilon} e^{-i\varepsilon\tau} \langle f' | \varepsilon \rangle \langle \varepsilon | f \rangle$ with $|\varepsilon\rangle \langle \varepsilon|$ expanded by Eq. (S7) as:

$$\begin{aligned} |\varepsilon\rangle \langle \varepsilon| &= |\varepsilon_0\rangle \langle \varepsilon_0| \\ &+ (t/V) \cdot (|\varepsilon_0\rangle \langle \varepsilon_1| + |\varepsilon_1\rangle \langle \varepsilon_0|) \\ &+ (t/V)^2 \cdot (|\varepsilon_1\rangle \langle \varepsilon_1| + |\varepsilon_0\rangle \langle \varepsilon_2| + |\varepsilon_2\rangle \langle \varepsilon_0|) \dots \end{aligned} \quad (\text{S11})$$

Consider $\langle f' | \varepsilon \rangle \langle \varepsilon | f \rangle$ and $|f\rangle \in \{l_0\}$, if $|f'\rangle \notin \{l_0\}$ then $|\varepsilon_0\rangle \langle \varepsilon_0|$ yields zero, thus $|\varepsilon\rangle \langle \varepsilon|$ and $\langle f' | f(\tau) \rangle \sim \mathcal{O}(t/V)$. However, if $|f'\rangle \in \{l_0\}$, as discussed in Sec. IIB, $|\varepsilon_0\rangle \langle \varepsilon_1|$ and $|\varepsilon_1\rangle \langle \varepsilon_0|$ result in zeros. Then $|\varepsilon\rangle \langle \varepsilon| \sim |\varepsilon_0\rangle \langle \varepsilon_0| + (t/V) (|\varepsilon_0\rangle \langle \tilde{\varepsilon}_2| + |\tilde{\varepsilon}_2\rangle \langle \varepsilon_0|)$, where $|\tilde{\varepsilon}_2\rangle$ represents the part of $|\varepsilon_2\rangle$ recovering l_0 . As a result, $\langle f' | f(\tau) \rangle \sim \mathcal{C}(\tau) + (t/V) \mathcal{F}(\tau)$, where $\mathcal{C}(\tau) = \sum_{\varepsilon} e^{-i\varepsilon\tau} \langle f' | \varepsilon_0 \rangle \langle \varepsilon_0 | f \rangle$ describes the singlon motions that conserve the NN links and the singlons, and $\mathcal{F}(\tau) = \sum_{\varepsilon} e^{-i\varepsilon\tau} (\langle f' | \varepsilon_0 \rangle \langle \tilde{\varepsilon}_2 | f \rangle + \langle f' | \tilde{\varepsilon}_2 \rangle \langle \varepsilon_0 | f \rangle)$ describes the dynamics that conserve only the NN links.

The observables characterized by $|\langle f' | f(\tau) \rangle|^2$ exhibit the following behavior: if $|f\rangle$ and $|f'\rangle$ possess the same number of NN links, then the observable scales as $|\mathcal{C}|^2 + \mathcal{O}(t/V)$, otherwise it scales as $\mathcal{O}(t^2/V^2)$. Thus, the dynamics are grounded by the initial NN links to the order of (t/V) , even as the singlon number may evolve. In the main text, we consider a total of Ω_0 Fock states $|f_0\rangle$ with $\langle f_0 | \hat{n}_j | f_0 \rangle = 1$ and compute $\eta(\tau)$ averaged over $|f_0\rangle$. Since $\eta(\tau) \propto \frac{1}{\Omega_0} \sum f_0, f'_0 |\langle f'_0 | f_0(\tau) \rangle|^2 \sim \frac{1}{\Omega_0} \sum f_0, f'_0 |\mathcal{C}(\tau) + (t/V) \mathcal{F}(\tau)|^2$, expanding to first order in (t/V) yields the expressions of $A(\tau)$ and $B(\tau)$ utilized in the main text. Given that they both stem from the processes conserving the NN links, we simplify $B \sim A + \epsilon$.

-
- [1] L. Šamaj and Z. Bajnok (2013), *Introduction to the Statistical Physics of Integrable Many-body Systems*
[2] J. J. Sakurai and J. Napolitano (2010). *Modern Quantum Mechanics* (2nd ed.)
[3] L. D. Landau, E. M. Lifschitz (1977). *Quantum Mechanics:*

Non-relativistic Theory (3rd ed.)